

Chapter 3

Journal of Applied Electrochemistry
<https://doi.org/10.1007/s10800-023-01938-4>

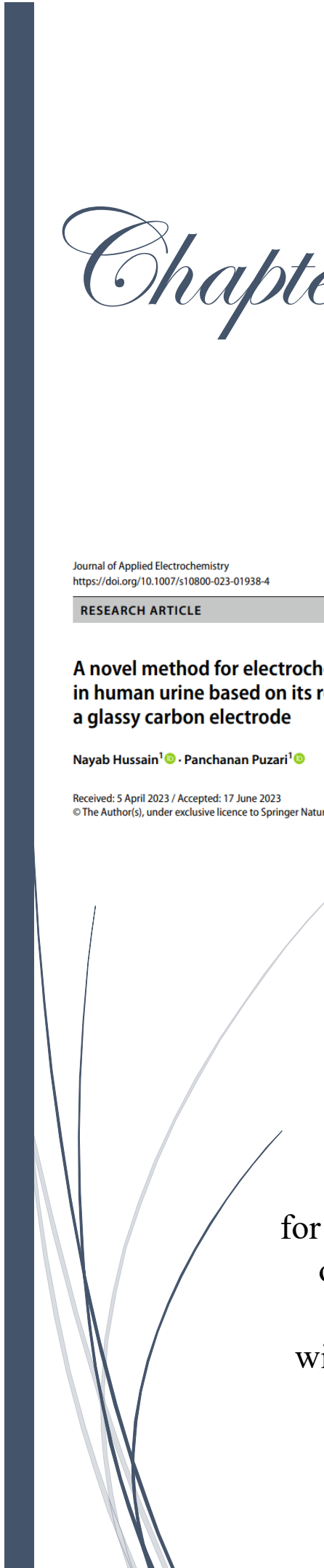
RESEARCH ARTICLE



A novel method for electrochemical determination of creatinine in human urine based on its reaction with 2-nitrobenzaldehyde using a glassy carbon electrode

Nayab Hussain¹ · Panchanan Puzari¹

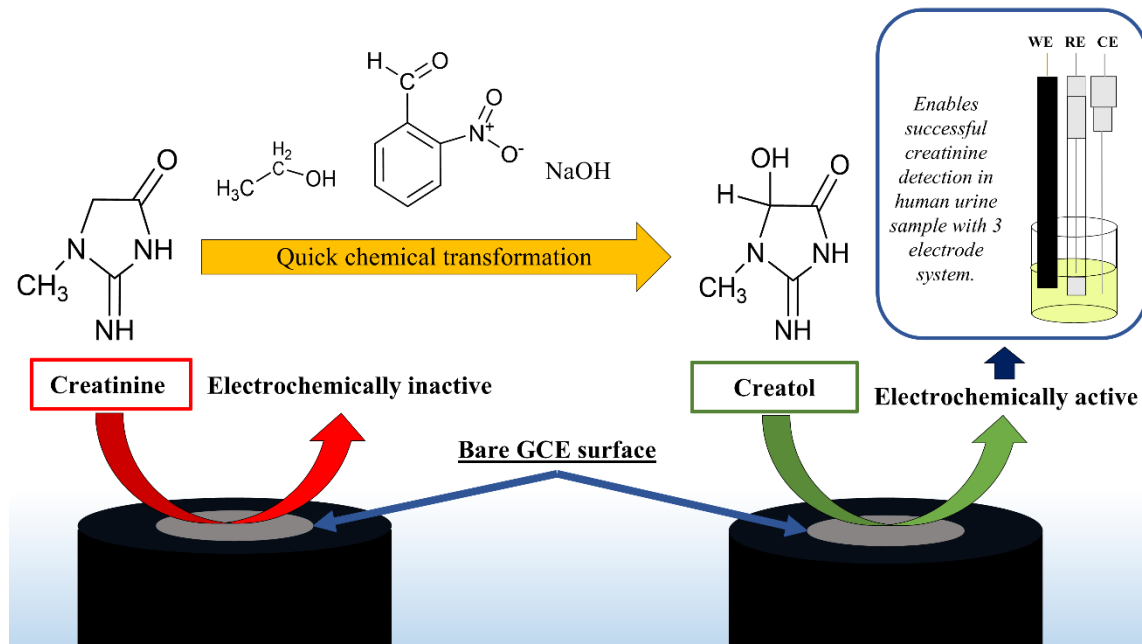
Received: 5 April 2023 / Accepted: 17 June 2023
© The Author(s), under exclusive licence to Springer Nature B.V. 2023



A novel method
for electrochemical determination
of creatinine in human urine
based on its reaction
with 2-nitrobenzaldehyde using
a glassy carbon electrode

Highlights

Based on creatinine reaction with 2-nitrobenzaldehyde, an electrochemical non-enzymatic method for the sensitive determination of creatinine is reported in this chapter. The DPV technique was employed to demonstrate the sensing protocol. A plausible reaction mechanism has been proposed and successful application of this method for creatinine determination in a real sample (human urine) was also demonstrated. The mechanism indicated the formation of multiple electroactive species in the process. The linear range of detection was determined to be 1–25 mM, with an LOD of 0.50 mM and an excellent R^2 value of 0.99, which made the system suitable for creatinine determination in human urine. Interference studies were carried out with urea, uric acid, glucose, ascorbic acid and dopamine, and the interference percentages were determined to be within the acceptable limit. All the components except uric acid showed an interference of less than 3.2%, while uric acid showed a maximum interference of 8.4%. Its robustness, high selectivity, good sensitivity, and low detection limit project it as a promising new tool for a point-of-care testing device.



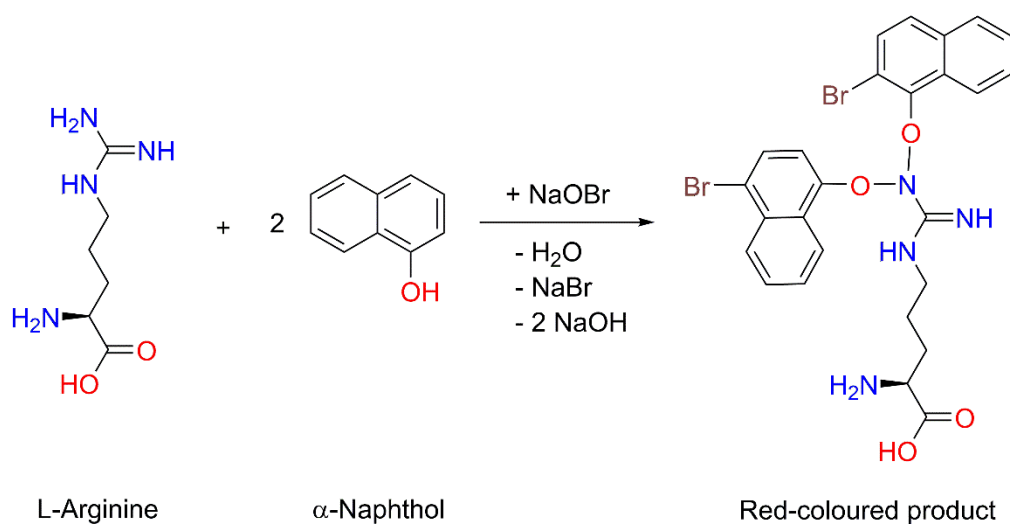
This part of the thesis is published as:

Hussain, N. and Puzari, P. A novel method for electrochemical determination of creatinine in human urine based on its reaction with 2-nitrobenzaldehyde using a glassy carbon electrode. *Journal of Applied Electrochemistry*, 54(1):75–187, 2024.

3.1 Introduction

One of the established non-enzymatic electrochemical creatinine determination techniques involves the formation of its electroactive complexes by coordination with metal ions [1-11]. As the conversion of creatinine to an electroactive species is the prime requisite of such methods, it dawned upon us that creatinine can also be electrochemically determined by chemically transforming it into an electroactive species in a metal-free condition. Hence, we embarked on a new approach, which can be based on the utilization of electrochemical properties of the reaction products of creatinine with organic reactants.

On perusing the literature, we came across some interesting reports from the mid-20th century on the non-enzymatic transformation of creatinine to other products such as substituted guanidines. In 1939, *Riegert* [12] reported a colorimetric detection of creatinine by converting it to methyguanidine by applying heat, in the presence of HgO and alkali, followed by using the Sagakuchi colour reaction. This colour reaction was described by *Shoyo Sakaguchi* [13] and it's based on the reaction of L-arginine (which contains a guanidinium group) with the 'Sagakuchi reagent' (α -Naphthol and NaOBr) to give a red-coloured compound, as shown in Scheme 3.1.



Scheme 3.1: Sagakuchi colour reaction.

In 1956, *Pilsum et al.* [14] reported an improved version of the creatinine-to-methylguanidine conversion reaction, using additional reagents and controlled steps. The modified method involved three steps: a) oxidation of creatinine in phosphate buffer-H₂SO₄ solution to oxalylmethylguanidine (2-imino-1-methyl-imidazolidine-4,5-dione) in

the presence of 2-nitrobenzaldehyde (2-NBA) and NaOH, b) degradation of oxalylmethylguanidine to methylguanidine by hydrolysis with the application of heat, and c) determination of methylguanidine by modified Sakaguchi method [14]. Formation of methylguanidine has also been reported by oxidation of creatinine adsorbed on charcoal [15] and by air oxidation of creatinine in the presence of HCl [16] but those were comparatively time-consuming processes.

As our primary focus was on the quicker chemical transformation of creatinine to preferably an electrochemically active species, the ‘Step a’ of Pilsum’s method, that is, creatinine’s reaction with 2-NBA and NaOH, drew our attention. The above-mentioned chemical oxidation process of creatinine hasn’t been studied electrochemically. Hence, in this chapter, we initially investigated the electrochemical response of this reaction. The peculiar electrochemical response which shows a quantitative relation with creatinine concentration, encouraged us to optimize the conditions and develop a non-enzymatic method for quantitatively determining creatinine. This method leads to easy and cost-effective electrochemical determination of creatinine using a bare GCE. Furthermore, a plausible mechanism for the reaction and designations of the redox processes has also been proposed.

3.2 Experimental

3.2.1 Chemicals, reagents and instruments

Creatinine was purchased from Alfa Aesar; potassium dihydrogen phosphate from Rankem; dipotassium hydrogen orthophosphate, urea (extra pure) and 2-nitrobenzaldehyde (extra pure analytical reagent) from SRL; sodium hydroxide pellets, ethanol, glucose and potassium chloride from Merck; uric acid, ascorbic acid and dopamine from Sigma-Aldrich. All these chemicals were of analytical grade and used without purification.

Biologic SP-300 with EC-lab software setup was used for electrochemical analysis and Perkin Elmer Frontier MIR-FIR for FTIR spectroscopy.

3.2.2 Solution preparation

Creatinine solutions (CRS) were prepared in 0.1 M PBS. 7 % 2-NBA solution was prepared by dissolving 7 mg of solid 2-NBA in 100 μ L ethanol and 1.25 N NaOH solution was prepared in Milli-Q water.

In this chapter, the mixture of PBS, 1.25 N NaOH solution and 7 % 2-NBA solution is abbreviated as PBS/NaOH/2-NBA or called the ‘blank solution’. The mixture of CRS, 1.25 N NaOH solution and 7 % 2-NBA solution is abbreviated as CRS/NaOH/2-NBA or called the ‘test solution’. Both blank and test solutions were prepared in the same volume ratio, i.e., 100:10:1.

3.2.3 Electrochemical and spectroscopic procedures

For electrochemical analyses, 10 μ L of 2-NBA solution and 100 μ L of NaOH were added to 1000 μ L of PBS (in case of blank solution analysis), CRS or human urine sample, and transferred to the electrochemical cell for the analyses.

DPV and CV techniques were used to determine a plausible mechanistic pathway of the reaction between creatinine and 2-NBA in the presence of NaOH. FTIR and UV-vis spectroscopy were also used to gather evidence for the reaction mechanism. Optimization of parameters, determination of the limit of detection (LOD) of creatinine based on the reaction, interference study and real medium (urine) analysis were carried out using the DPV technique only. For all the electrochemical analyses, a well-polished bare glassy carbon electrode (GCE) was used as the working electrode, Ag/ AgCl/KCl (3.5 M) as the reference electrode and Pt wire as the counter electrode. DPVs were recorded from -1.0 V to 0.5 V with a pulse height of 2.5 mV, pulse width of 100 ms, step height of 5.0 mV and step time of 500 ms. CVs were recorded in the potential range of -1.0 V to 0.5 V, with a scan rate of 0.1 V s^{-1} . FTIR spectra were recorded in the wavenumber range of 4000 cm^{-1} to 400 cm^{-1} .

3.2.4 Optimization of the reaction parameters

pH and reaction time were optimized, before proceeding to the determination of LOD, interference and real medium study. Optimization of pH was carried out by recording the DPVs for a series of test solutions, each containing 25 mM CRS, but different pH of the buffer. The test solutions were gently stirred after mixing and incubated for 600

s before recording their DPVs. The baseline currents were determined by recording triplicate DPVs for the corresponding blank solutions. The optimum pH for the reaction was determined from the graph of average peak currents and baseline currents plotted against the respective pH of the buffer.

Test solutions containing 25 mM CRS, having the previously optimized pH, were prepared to optimize the reaction time. DPVs were recorded for the test solutions after different reaction times (from 30 to 1500 s). The optimum reaction time was determined from the graph of peak currents plotted against reaction time.

3.2.5 Electrochemical determination of creatinine and LOD calculation of the system

Triplicate DPVs were recorded at the optimum conditions, for test solutions having different concentrations of creatinine. A calibration curve was plotted for the average oxidative peak currents against the creatinine concentrations. Triplicate DPVs were also recorded for the blank solution to determine the average current and standard deviation in the absence of the analyte. The unknown concentration of creatinine in real media can be determined from the calibration curve and the LOD of the system was then determined using Equation 3.1 where ‘Sb’ is the standard deviation of the blank, and ‘m’ is the slope obtained from the calibration curve.

$$\text{LOD} = 3 \left(\frac{\text{Sb}}{m} \right) \quad (\text{Eq. 3.1})$$

3.2.6 Interference

Possible interference by other urinary components, such as urea, uric acid, glucose, ascorbic acid and dopamine, has been investigated. Triplicate DPVs of test solutions in the presence of different concentrations of each of the possibly interfering species mentioned above were recorded at the optimum conditions. The test solutions were prepared containing 5 mM CRS and the same pH of the buffer (6.6). The percentage of interference was calculated as the percentage change between the initial peak current, A (in the absence of interfering species), and the final peak current, B (in the presence of interfering species), using Equation 3.2.

$$\text{Interference percentage} = \left(\frac{|A - B|}{A} \right) \times 100 \%$$

(Eq. 3.2)

3.2.7 Urine sample

A urine sample for analysis was collected from a volunteer student. After 2-fold dilution with PBS and adjusting urinary pH to our optimized value, 1 ml of the urine sample was placed in the electrochemical cell after filtering with a syringe filter, followed by the addition of 100 μL NaOH and 10 μL 2-NBA. Triplicate DPVs of the reagents-mixed urine sample were recorded at optimized reaction time. The process was then repeated for 1 ml of urine samples spiked with different concentrations of creatinine. From the obtained average oxidative peak currents, creatinine concentration in raw urine was calculated by considering the dilution factor and the recovery percentages were also obtained.

3.3 Results and Discussion

3.3.1 Electrochemical behaviour

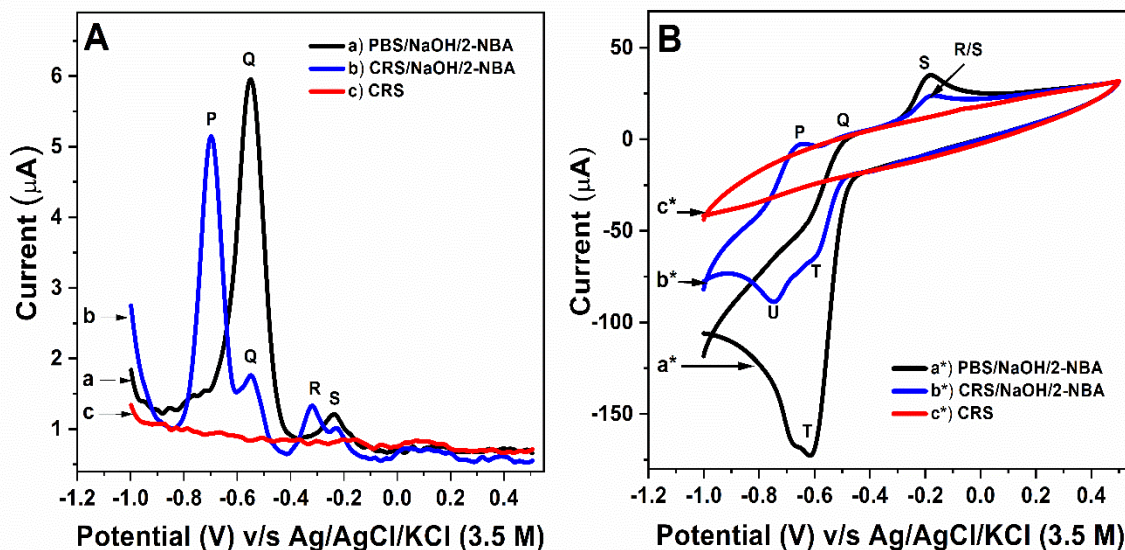


Figure 3.1: A) DPVs obtained for (a) blank solution (PBS/2-NBA/NaOH), (b) test solution (CRS/2-NBA/NaOH) containing 25 mM creatinine in the added CRS and (c) 25 mM creatinine solution (CRS) B) a*, b* and c* are their respective cyclic voltammograms.

Electrochemical behaviour was studied by comparing DPVs and CVs obtained in the same pH for the blank, test and creatinine solution. In Figure 3.1 (A), it can be seen in curve 'c' that no redox peak was obtained for the creatinine solution, while two oxidation peaks Q (− 0.53 V) and S (− 0.23 V) were observed in the DPV of the blank solution (curve a). In the DPV of the test solution (curve b), while the intensity of 'peak Q' was considerably inhibited, the same of 'peak S' was not significantly affected. In addition, two new oxidation peaks, P (− 0.69 V) and R (− 0.31 V), appeared in the voltammogram. A similar trend could be observed in the CVs obtained for the test solution, blank solution and creatinine solution, as can be seen in Figure 3.1 (B). In addition to the reduction peak, T, obtained for both the blank solution (curve a*) and test solution (curve b*), another reduction peak, U, was generated for the test solution (curve b*) as can be seen in their CVs [Figure 3.1 (B)]. The occurrence of all these peaks is further explained in detail in Section 3.3.9. However, the generation of the new peaks (P, R and U) and the inhibition of the native peaks (Q, S and T) in the test solution were indications of a certain reaction between creatinine and 2-NBA in the presence of NaOH. Only the prominent peaks, P and Q, were taken into consideration for further analysis using DPV. The processes giving rise to each peak, and corresponding equations, are explained in Section 3.3.9.

3.3.2 Kinetic model of the system

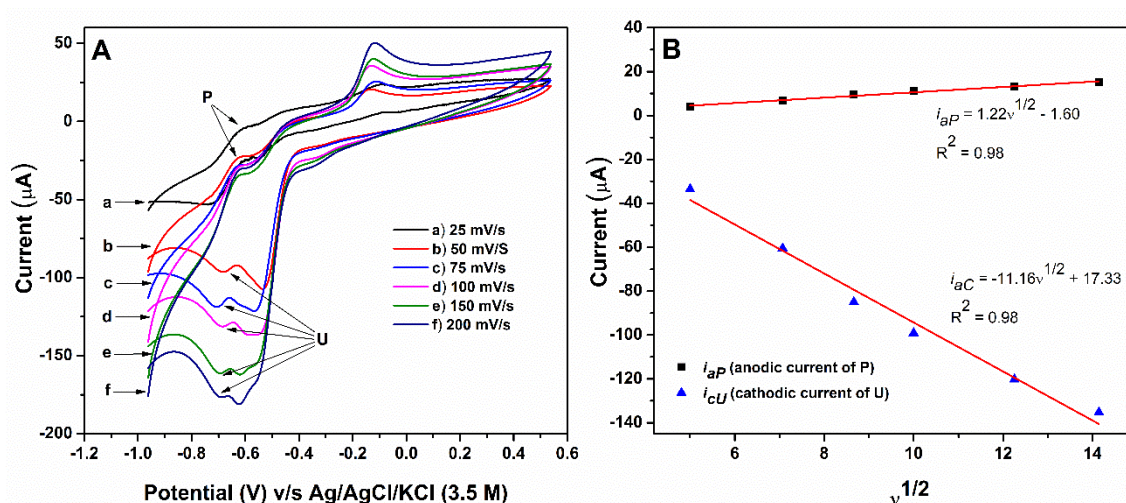


Figure 3.2: A) CVs obtained for test solutions with the scan rate a) 25 mV/s, b) 50 mV/s, c) 75 mV/s, d) 100 mV/s, e) 150 mV/s and f) 200 mV/s. B) Plot of the anodic peak current (i_{aP}) and the cathodic peak current (i_{cU}) against the square root of the scan rate ($v^{1/2}$).

The voltammogram responses at varying scan rates were analyzed to determine the kinetic model of the system. Test solutions with 25 mM creatinine in the added CRS were prepared, having the same pH of the buffer (6.6). After 600 seconds of reaction time, CVs were recorded for the test solutions at different scan rates, as shown in Figure 3.2 (A).

The oxidation peak P and reduction peak U are the prominent characteristic peaks generated in the presence of creatinine. Thus, the anodic current corresponding to peak P (i_{aP}) and the cathodic current corresponding to peak U (i_{cU}) were plotted against the square root of the scan rate ($v^{1/2}$) to study the kinetics. Figure 3.2 (B) shows the variation of i_{aP} and i_{cU} with $v^{1/2}$. It can be seen in the figure that both anodic peak current and cathodic peak current displayed linearity when plotted against the square root of the scan rate, and have very good R^2 values of 0.98 each. This study inferred that it is largely a diffusion-controlled process.

3.3.3 Selection of reagent parameters and validating 2-NBA concentration

To 1000 μ L of PBS or CRS, 100 μ L of 1.25 N NaOH and 10 μ L of 7 % (w/v) 2-NBA solution were added to prepare the blank and the test solution respectively. The concentrations of NaOH and 2-NBA solution have been maintained as mentioned in the pioneering work by *Pilsum et al.* [3]. As the reaction proceeds in an alkaline condition, the volume ratio of 10:1 for PBS:NaOH or CRS:NaOH was selected to ensure the alkalinity of the resulting mixture, irrespective of the pH of the buffer. However, the volume of the added 2-NBA solution was chosen arbitrarily. Hence, there was a need to validate the 2-NBA concentration in this study.

Test solutions containing 25 mM CRS were prepared, having the same pH of buffer (6.6) but with different concentrations of the added 2-NBA solution. After 600 s of reaction time, triplicate DPVs were recorded for each test solution. Figure 3.3 (A) shows a set of the DPVs for the test solutions with varying 2-NBA concentrations.

Figure 3.3 (B) shows a graph of the average oxidative peak currents (P and Q) plotted against the 2-NBA concentrations. It can be seen in the figure that the average peak current of Q increased with the increase in the 2-NBA concentration. However, the average peak current of P initially increased as we increased the concentration of 2-NBA from 2% to 7% and reached saturation thereafter. It can be inferred from this study that, as Q is the native peak of 2-NBA (explained in detail in Section 3.3.9), it was expected to increase

with the increase in the 2-NBA concentration. However, the occurrence and intensity of peak P depend on the creatinine concentration in the test solution. For any fixed amount of creatinine, a 7% concentration of 2-NBA was optimum to carry out the electrochemical analysis, without any waste of chemicals.

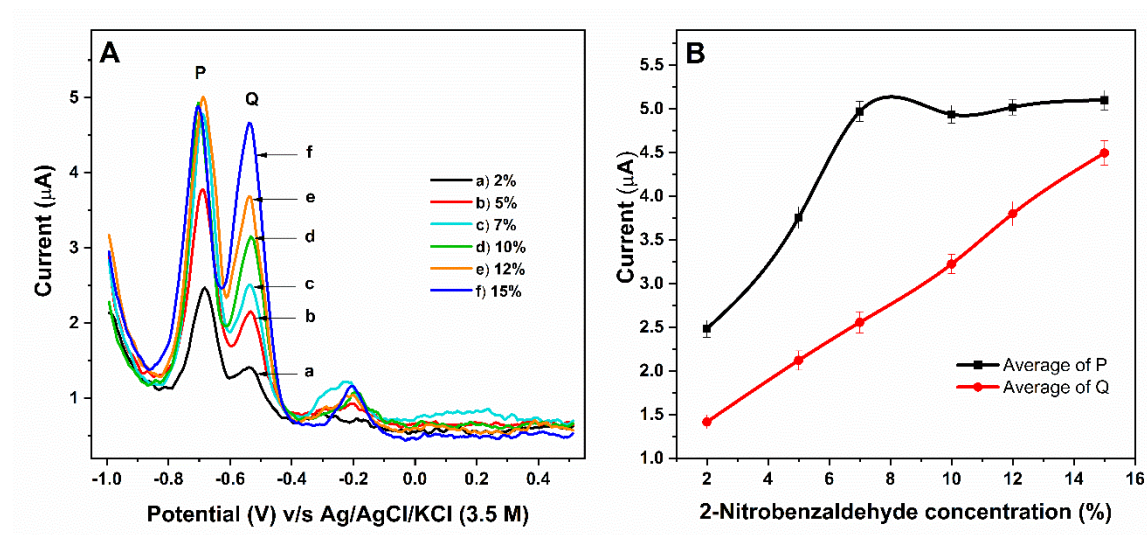


Figure 3.3: A) DPVs obtained for test solutions with the concentration (w/v) of the added 2-NBA solution being a) 2 %, b) 5 %, c) 7 %, d) 10 %, e) 12 % and f) 15 %. B) Plot of average oxidative peak currents (P and Q) obtained for test solutions against different concentrations of 2-NBA.

3.3.4 pH optimization

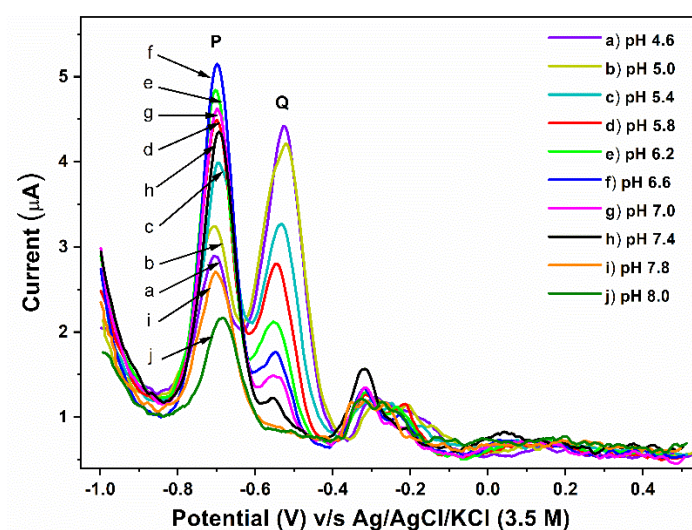


Figure 3.4: DPVs obtained for test solutions when the pH of the buffer was (a) 4.6, (b) 5.0, (c) 5.4, (d) 5.8, (e) 6.2, (f) 6.6, (g) 7.0, (h) 7.4, (i) 7.8 and (j) 8.0.

The effect of pH on the oxidation peaks P and Q were studied with the DPV technique by varying the pH range from 4.6 to pH 8.0, as shown in Figure 3.4. The pH range of 4.6 to 8.0 was selected considering that the pH of a normal urine sample is approximately 6.0 [17]. Peak current at a pH was recorded at the reaction time of 600 s.

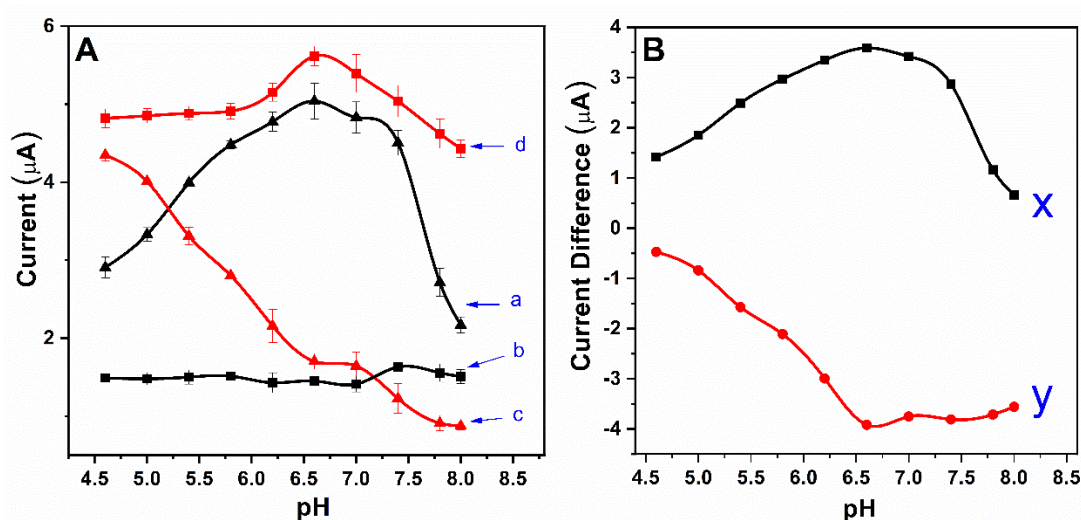


Figure 3.5: A) Plot of average oxidative peak current of peak P (curve a) and average oxidative peak current of peak Q (curve c) for test solutions; plot of average baseline current for P (curve b) and average initial blank oxidation peak current for Q (curve d) for blank solutions, against the pH of the buffer. B) Plot of the current difference in the DPVs of the test and the blank solutions with reference to peak P (curve x) and peak Q (curve y) at different pH, after 600 s of reaction time.

The curve 'a' in Figure. 3.5 (A) shows that the peak current of P increased with the increase in pH of the buffer from 4.6, reached a maximum at pH 6.6, and decreased thereafter with a further increase in the pH. In the case of peak Q (curve c), the intensity decreased almost linearly throughout the pH range from 4.6 to 8.0. It was to be noted that curve 'd' represents oxidative peak currents obtained at -0.53 V owing to the maximum oxidation of protonated 2-nitrobenzaldehyde in the absence of creatinine (refer to Section 3.3.9). The obtained trend indicated that in the absence of creatinine, electrochemical oxidation of protonated 2-NBA was highest at pH = 6.6 of the buffer solution. Similarly, getting a maximum at 6.6 in the case of curve 'a' indicated that the oxidation of a

transformed product of creatinine (creatol; refer to section 3.3.9) also occurred to a maximum extent at pH 6.6.

Figure 3.5 (B) shows the current difference between the test and the blank run for both the peaks in the selected pH range. As expected, the variation pattern was maximum at pH 6.6, thus indicating that the pH of 6.6 was the ideal pH for quantitative estimation of creatinine

3.3.5 Optimization of reaction time

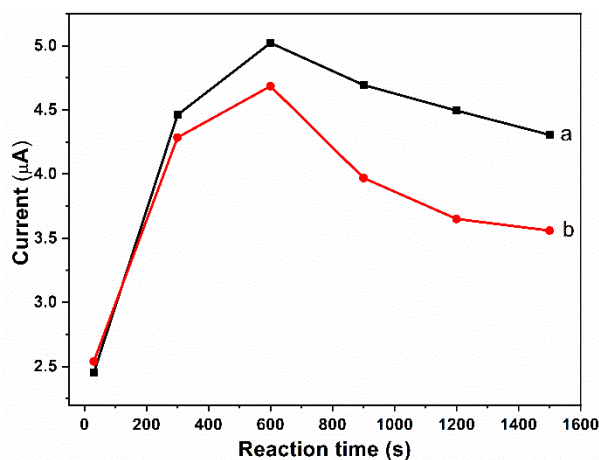


Figure 3.6: Time variation of the oxidative current of peak P in test solutions when the pH of the buffer was (a) 6.6 and (b) 7.4.

DPVs were recorded for test solutions, having equal creatinine concentration but different pH of buffer (6.6 and 7.4). The oxidation peak P, which occurs only in the presence of creatinine in the system, was analysed to determine the optimum reaction time. It can be seen in Figure 3.6 (curve a) that the intensity of peak P initially increased with time up to 600 s, following which the intensity decreased. This inferred that the optimum reaction time was 600 s. When the pH of the buffer was 7.4, the peak current variation followed the same trend, as seen in curve 'b', thus indicating that the optimum reaction time was pH-independent.

3.3.6 Determination of the LOD

Figure 3.7 (A) represents the DPVs obtained for test solutions having the same pH of buffer but different creatinine concentrations (from 1 to 100 mM) in the added CRS. The first oxidation peak P was considered to determine the LOD of the system.

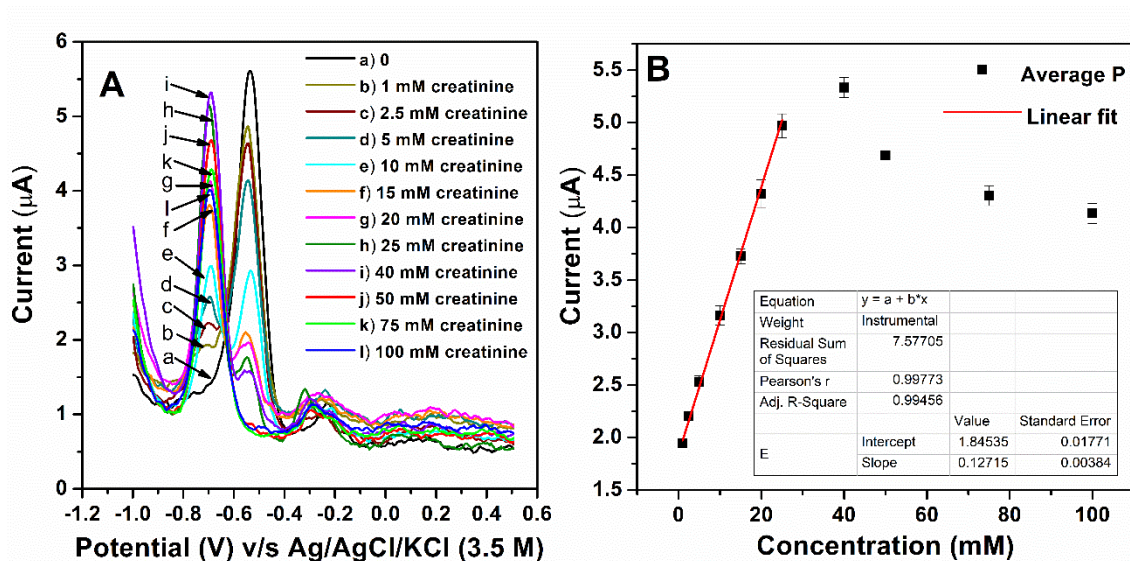


Figure 3.7: A) DPVs obtained for (a) blank solution and (b–l) test solutions containing different CRS concentrations. B) Calibration curve obtained by plotting average oxidative peak currents (n = 3) of P against the concentrations of creatinine.

From the plot of average oxidative peak currents of P against the concentrations of creatinine, as can be seen in Figure 3.7 (B), it was evident that at higher concentrations (above 25 mM) the calibration curve deviated from linearity. This deviation can be attributed to the hindrance caused by the unreacted creatinine to the electrochemical oxidation of creatol at the electrode surface (refer to Section 3.3.9). However, the linear fit from 1 mM to 25 mM had an excellent R^2 value of 0.99 with a slope (m) of 0.12 and an intercept of 1.84. The linear fit is represented by Equation 3.3, where y is the current response (in μA) and x is the creatinine concentration (in mM).

$$y = 0.12x + 1.84$$

(Eq. 3.3)

The standard deviation (Sb) for the blank solution was calculated to be 0.02. Thus, the LOD of this system for the concentration range below 25 mM was determined to be 0.50 mM. Hence, this reported system for creatinine determination well-covered the concentration range for the determination of urinary creatinine levels.

A comparison of the linear range of detection, R^2 value and LOD of our method with that of some other reported methods of urinary creatinine detection has been tabulated in Table 3.1.

Table 3.1: Comparison of performance of our method with some other urinary creatinine detection methods.

Sl. No.	Method	Linear range of detection (mM)	R^2 Value	LOD (mM)	Reference
1.	Capillary zone electrophoresis	0.2-32	0.99	0.05	[18]
2.	Colorimetric paper-based sensor using 3,5-dinitrobenzoate	0.82-10.0	0.99	0.27	[19]
3.	Colorimetric paper-based sensor using Jaffe method	1.05-20.0	0.99	0.35	[19]
4.	Square wave voltammetry using preanodized screen printed electrode	0.37-3.6	0.99	0.86×10^{-2}	[20]
5.	Chronoamperometry using carbon printed electrodes layered with FeCl_3 and cotton fiber	0.88-21.65	0.91	-	[11]
6.	Chronoamperometry using copper-electrodeposited gold electrode	Up to 12.6	0.99	0.05	[6]
7.	Differential pulse voltammetry using bare glassy carbon electrode	1-25	0.99	0.50	This work

3.3.7 Interference study

Next to water, which constitutes about 95% of urine, the most abundantly found urine component is urea. While urea in blood ranges from 2.6 mM to 6.5 mM, its concentration in urine can be about 50 times higher [21] i.e., approximately in the range

of 130 mM to 325 mM. The normal range of all other components in urine is much smaller. The normal glucose concentration must be below 15 mg/dL (0.8 mM) [22], ascorbic acid concentration in a number of normal individuals was reported to be roughly in the range of 0.11 mM to 0.17 mM but could get a little higher or lower under certain conditions [23], and, normal dopamine concentration ranges from 0.0003 mM to 0.00313 mM [24]. *Iwata et al.* [25] reported that the solubility of uric acid increases with the rise in pH of solutions; for solutions with pH up to 7.0, the maximum solubility of undissociated uric acid was found to be 0.35 mM and thereafter, its solubility solely relied on the increase of urate ions formed by its dissociation. It was also found in the work reported by *Chauhan et al.* [26] that the uric acid level in the urine of healthy adults ranges from 0.16 mM to 0.32 mM with a mean of 0.21 mM, as was measured by their uricase nanoparticles/Au electrode. Interference imposed in this creatinine detection system by all the above-mentioned urinary components was studied, considering their solubility in our working pH and by varying their concentration within their normally found range in human urine.

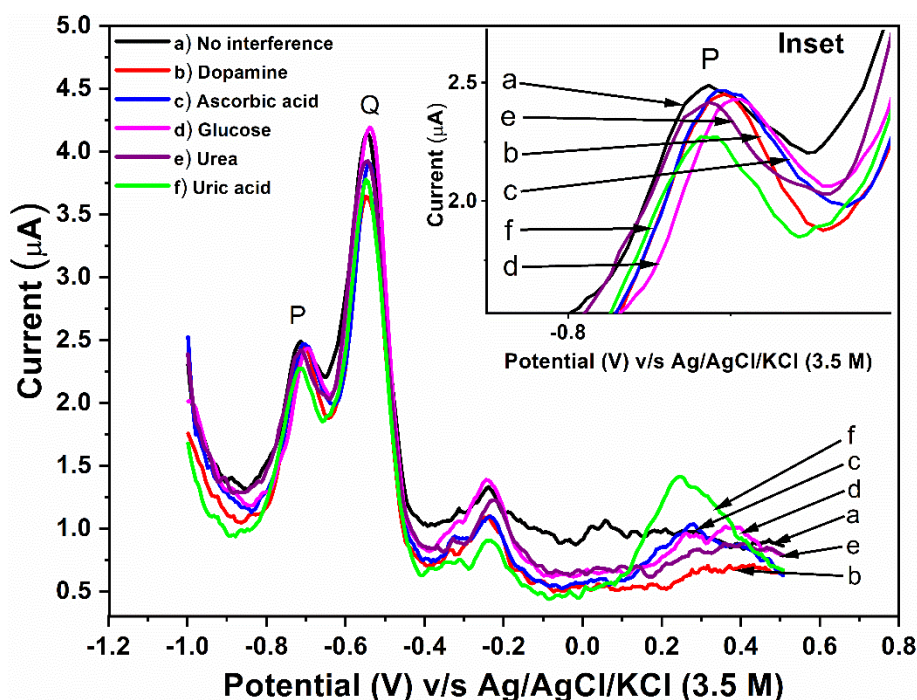


Figure 3.8: DPVs obtained for test solutions in the presence of (a) no interference, (b) dopamine (0.003 mM), (c) ascorbic acid (0.3 mM), (d) glucose (0.8 mM), (e) urea (250 mM) and (f) uric acid (0.3 mM).

(Inset: Enlarged view of the oxidation peak P).

After 600 s of reaction time, the average oxidative peak current of P for a test solution was determined in the absence of the interfering species. The same was then determined in the presence of different concentrations of urea, uric acid, glucose, ascorbic acid and dopamine. The percentage of interference was determined by the percentage change in the average oxidative peak currents of P in the presence and absence of the other urinary components, using Equation 3.2. The signal responses are shown in Figure 3.8 and the values are shown in Table 3.2.

Table 3.2: Percentage of interference to the analytical signal by different concentrations of urinary components.

Solution	Concentration of the added component to CRS (mM)	Average oxidative peak current of P (μA)	Relative standard deviation (%)	Percentage of interference
Test solution (TS)	0	2.52 ± 0.007	0.27	-
TS + Urea	150	2.51 ± 0.05	1.99	0.58 %
	200	2.46 ± 0.09	3.65	2.48 %
	250	2.45 ± 0.04	1.63	3.12 %
TS + Uric acid	0.1	2.49 ± 0.03	1.20	1.61 %
	0.2	2.35 ± 0.06	2.55	6.89 %
	0.3	2.31 ± 0.01	0.43	8.46 %
TS + Glucose	0.4	2.49 ± 0.11	4.41	1.55 %
	0.6	2.47 ± 0.13	5.26	2.44 %
	0.8	2.46 ± 0.09	3.65	2.76 %

TS + Ascorbic acid	0.1	2.53 ± 0.12	4.74	0.51 %
	0.2	2.52 ± 0.06	2.38	0.43 %
	0.3	2.51 ± 0.10	3.98	0.47 %
TS + Dopamine	0.001	2.52 ± 0.13	5.15	0.19 %
	0.002	2.53 ± 0.11	4.34	0.20 %
	0.003	2.52 ± 0.05	1.98	0.02 %

It was seen that all the interfering species tend to interfere by varying the intensity of the original peak current but to a negligible extent. Interference due to urea and glucose was found to be less than 3.15 %, while interference by ascorbic acid and dopamine was less than 0.55 %. The highest interference of just 8.46 % was shown by the presence of 0.3 mM uric acid, which was within the acceptable range (< 10 %).

It was also observed in Figure 3.8 that in the presence of uric acid, a well-defined oxidation peak occurred, centred around 0.24 V. This peak was found distinctly separated from the oxidation peak, P, thus indicating that this method of creatinine determination can also be further improved for simultaneous detection of urinary creatinine and uric acid.

3.3.8 Urine sample analysis

Two-fold dilution of the collected urine samples was carried out by adding PBS having a pH of 6.6 to the urine sample, meanwhile adjusting the pH of the urine sample to the optimum working pH of this system. 1 ml of the sample was then introduced to the electrochemical cell by injecting through a syringe filter, so as to filter out any precipitated or insoluble urinary component. Since it was known from our preliminary experiments that creatinine is highly soluble in PBS over the complete range of pH, it was unlikely to precipitate out and give us false results. To the filtered urine sample in the electrochemical cell, 100 μ L NaOH and 10 μ L of 2-NBA solution were added, and after 600 s of reaction time, DPVs were recorded. For analysis of the spiked urine sample, appropriate amounts of creatinine were added to the urine sample after filtration and the same procedure as mentioned above was followed. DPVs of the real sample analysis are shown in Figure 3.9 and the recovery data are shown in Table 3.3.

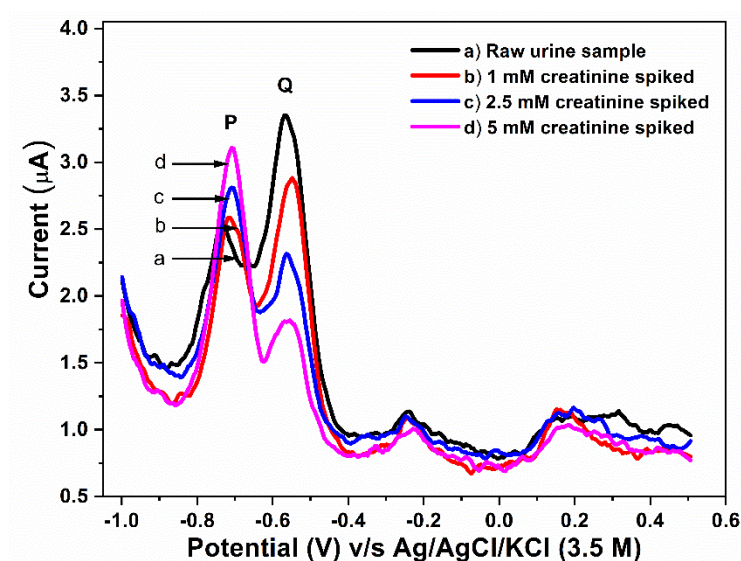


Figure 3.9: DPVs obtained for (a) raw urine sample and urine samples spiked with (b) 1 mM, (c) 2.5 mM and (d) 5 mM of creatinine, after the addition of NaOH and 2-NBA solution.

Table 3.3: Recovery percentage obtained for creatinine in a raw urine sample spiked with different concentrations of creatinine.

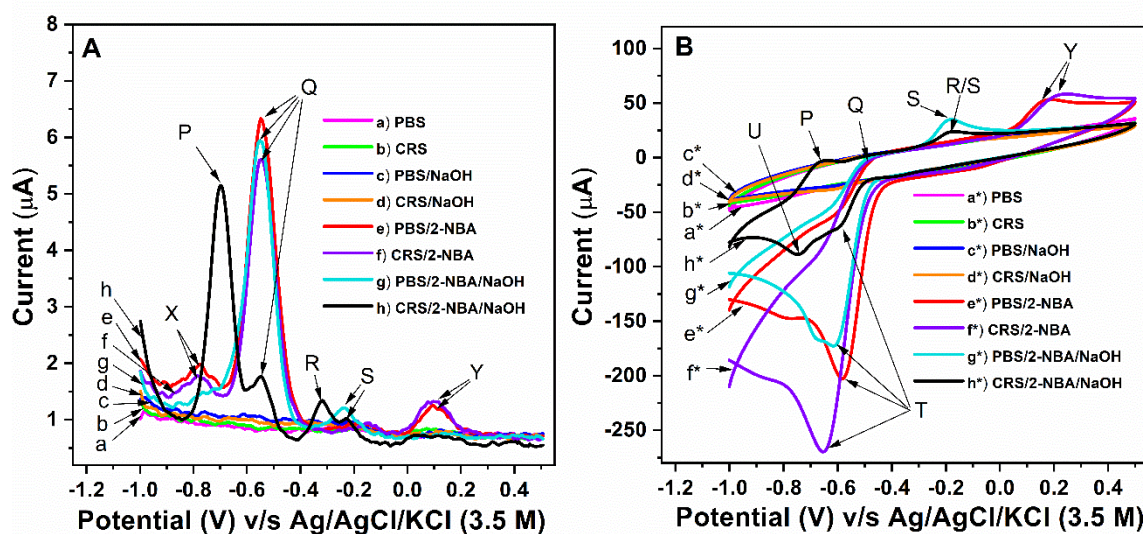
Spiked concentration (mM)	Obtained peak P current ($10^{-2} \mu\text{A}$)	Obtained concentration (10^{-2}mM)	A = Average obtained concentration (10^{-2}mM)	RSD (%)	E = Expected concentration (10^{-2}mM)	Average recovery percentage (%) = $(A/E) \times 100$ %
0	250.19	551.58	591.67	4.84		
	256.82	606.83				
	257.99	616.58				
1	264.81	673.42	664.14	5.21	691.67	96.02
	258.15	617.92				
	268.13	701.08				
2.5	283.43	828.58	816.94	2.99	841.67	97.06
	284.71	839.25				
	277.96	783.00				
5	313.49	1079.08	1147.81	4.76	1091.67	105.14

	322.19	1151.57				
	329.53	1212.75				

Figure 3.9 shows that the peak P appears distinctly in the raw urine sample and the peak current proportionately increases with an increase in the spiked creatinine concentrations. Excellent recovery between 96.02 and 105.14 % was obtained for the raw urine sample spiked with three different creatinine concentrations, as shown in Table 3.3. The average oxidative peak current of P for the raw urine sample was determined to be $2.55 \pm 0.04 \mu\text{A}$. Considering the dilution factor, the concentration of the collected urine sample was calculated to be 11.83 mM, which is within the normal urinary creatinine range [27, 28].

3.3.9 Discussion: a plausible mechanistic pathway of the reaction

3.3.9.1 Electrochemical perspective

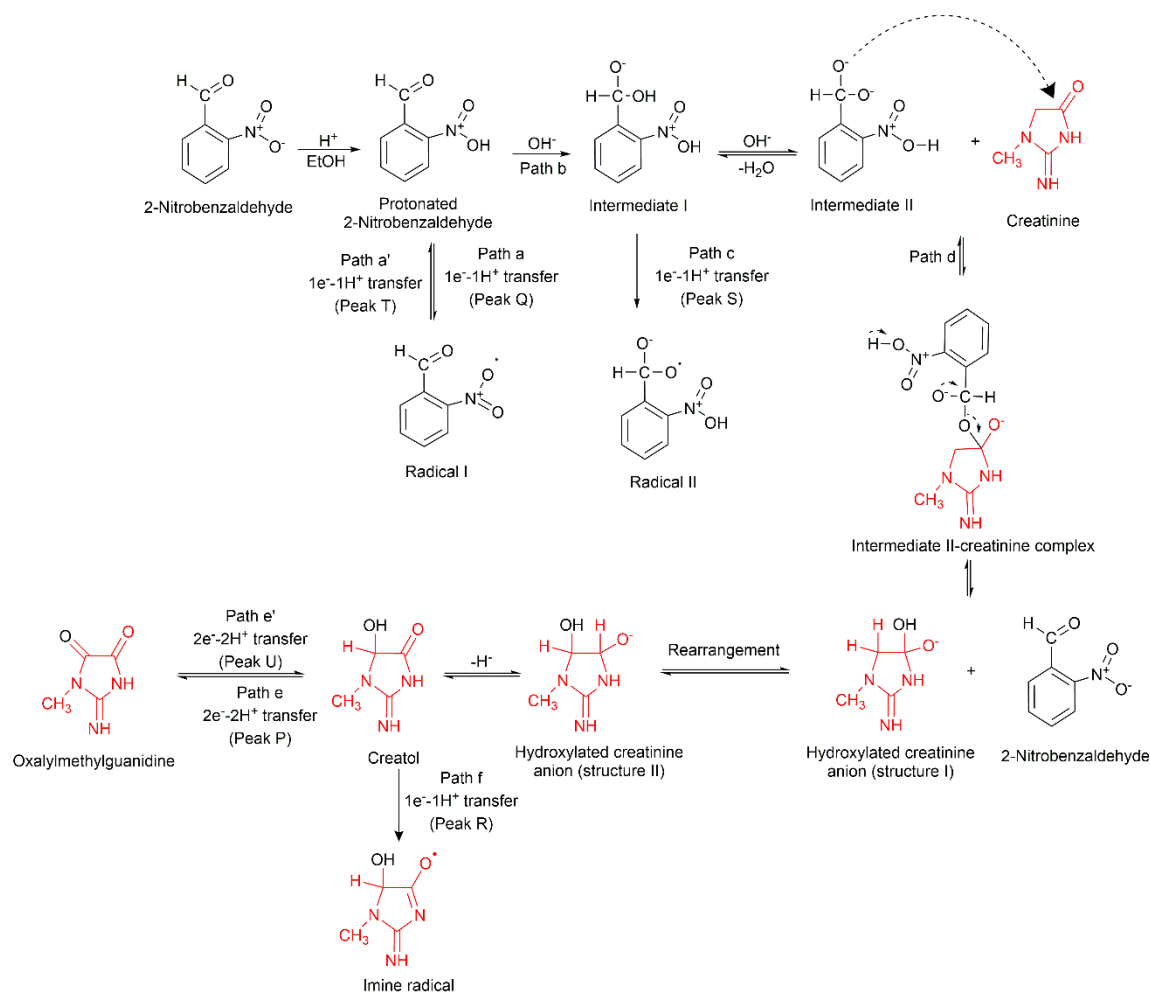


3.10: A) DPVs obtained for (a) PBS, (b) CRS, (c) PBS/NaOH, (d) CRS/NaOH, (e) PBS/2-NBA, (f) CRS/2-NBA, (g) PBS/2-NBA/NaOH (blank solution) and (h) CRS/2-NBA/NaOH (test solution). B) a*–h* are their respective cyclic voltammograms.

We tried to get an insight into the mechanism of the creatinine reaction with 2-NBA and the redox processes through a comparative study of CVs and DPVs of different solutions and solution mixtures (Figure 3.10). In Figure 3.10 (A), curve ‘a’ to ‘d’ represents

the DPVs of PBS, CRS, PBS/NaOH (mixture of PBS and NaOH in the volume ratio of 10:1) and CRS/ NaOH (mixture of CRS and NaOH in the volume ratio of 10:1), respectively. From these curves, it was evident that no oxidation peak was exhibited by these solutions and solution mixtures. In the DPV of PBS/2-NBA (mixture of PBS and 2-NBA in the volume ratio of 100:1), three oxidation peaks (X, Q, Y) were seen in the voltammogram (curve e). After replacing PBS with CRS in the above mixture (having the same volume ratio), resulting in CRS/2-NBA, we found that the voltammogram (curve f) was not affected. It implied that creatinine did not react with 2-NBA. Curve 'g' is the DPV of PBS/2-NBA/NaOH (blank solution) which was obtained by adding NaOH to PBS/2-NBA. As is evident from its voltammogram, the principal peak, Q, was not affected but suppression of the small peaks, X and Y, occurred. Along with that, there was a generation of a new small peak, S. After replacing PBS with CRS in the above mixture, resulting in CRS/2-NBA/ NaOH (test solution), it was seen that the peaks, X and Y, did not appear, Q and S got suppressed, and two new peaks, P and R, were generated, out of which the peak P appeared as the prominent one (curve h). Thus, from the comparison of curves 'f' and 'h', it was obvious that creatinine reacted with 2-NBA in the presence of NaOH and the reaction involved some redox processes.

The corresponding CV analyses are shown in Figure 3.10 (B). CVs of PBS, PBS/NaOH, CRS and CRS/NaOH (curve a*-d*) did not show any peak, which was in accordance with their respective DPVs. Three oxidation peaks (X, Q and Y) were expected from the CVs of PBS/2-NBA (curve e*) and CRS/2-NBA (curve f*), but only two oxidation peaks showed up, which corresponded to the peaks, Q and Y, in their respective DPVs. The small intensity peak, X, did not show up due to the lower resolution of the CV technique as compared to DPV. Similar to its DPV, in the CV of PBS/2-NBA/NaOH (curve g*), peak Q and the new peak, S, were also seen, while Y got suppressed. In the CV of CRS/2-NBA/NaOH, the new peak, P, was seen, reflecting similar results to that of its DPV, but again due to the lower resolution of the CV technique, the small peaks, R and S, were not easily distinguishable from each other and appeared to be merged (curve h*). Apart from the oxidation peaks, a reduction peak, T, was also observed in the curves 'e*' to 'h*' with varied intensity (intensity in curve f* > e* > g* > h*). In addition to T, another reduction peak, U, was observed specifically in curve 'h*'.



Scheme 3.2: Plausible mechanistic pathway of the reactions occurring in the test solution containing creatinine, 2-nitrobenzaldehyde/ethanol and NaOH.

The three oxidation peaks (X, Q and Y) obtained in the DPV of PBS/2-NBA (curve e) can be attributed to being the native oxidation peaks of 2-NBA. The electrochemical oxidation corresponding to the principal peak Q (− 0.53 V) can be attributed to the 1e⁻-1H⁺ oxidation occurring at the nitro group of the protonated 2-NBA to yield ‘Radical I’ as shown in Scheme 3.2 (path a). This can be substantiated by the literature report that protonation of nitro groups can be observed in protic solvents [29]. Hence, in a solution of 2-NBA in EtOH (a protic solvent), the nitro group can get protonated to produce the protonated 2-NBA which can readily undergo electrooxidation to produce ‘Radical I’. The other two small oxidation peaks of 2-NBA, X (− 0.8 V) and Y (1.0 V), can be attributed to the electron transfer occurring from its carbonyl group (C = O). This claim can be further

supported by the fact that on the addition of NaOH to PBS/2-NBA, unlike the principal peak Q, the minor peaks, X and Y, got completely inhibited as can be seen in the DPV and CV of PBS/2-NBA/ NaOH (curve g and g*, respectively). It was because of the nucleophilic attack of the dissociated hydroxyl ion (left after reaction with the weak acid of the buffer) at the carbonyl carbon, which eventually resulted in the formation of an 'Intermediate I' and 'Intermediate II' (as shown in Scheme 3.2 via 'path b') and thereby, hindered the electro-oxidation peaks, X and Y. However, since the nitro group of 2-NBA was unaffected by the addition of NaOH, electrochemical oxidation resulting in peak Q continued to occur from 'Intermediate I' and 'Intermediate II', via pathways similar to 'path a' in Scheme 3.2. Additionally, in curves 'g' and 'g*', a new oxidation peak, S, was generated which can be attributed to another electro-oxidation of the 'Intermediate I' to 'Radical II' by $1e^- - 1H^+$ transfer [Scheme 3.2 (path c)].

Peak Q remained unaffected until the formation of 'Intermediate II', but on replacing PBS with CRS in PBS/2-NBA/NaOH, resulting in CRS/2-NBA/NaOH, suppression of Q, as well as, simultaneous generation of well-defined oxidation peak, P (– 0.69 V) along with a small peak, R, was seen to occur (curve h and h*). This observation can also be explained by the plausible mechanistic pathway of creatinine reaction with 2-NBA in the presence of NaOH as shown in Scheme 3.2 via 'path d'. According to this mechanism, in the presence of creatinine, 'path b to d' of Scheme 3.2 becomes the dominating path and 'Intermediate II' participates in the oxidation of creatinine to creatol. A small fraction of 'Intermediate II' reverts back to 'Radical II' through 'path c' thus leading to a relatively smaller intensity peak, S. Thus, oxidation of the protonated 2-NBA to 'Radical I' (via 'path a' of Scheme 3.2) diminished, and consequently, Q got inhibited. Once creatol is formed in the process as shown, it undergoes electrochemical oxidation ($2e^- - 2H^+$) to produce oxalylmethylguanidine, thus generating the oxidation peak, P [Scheme 3.2 (path e)]. Furthermore, the occurrence of R (– 0.32 V) can be attributed to another route of creatol oxidation by the transfer of $1e^- - 1H^+$ to form an imine radical, as represented in Scheme 3.2 (path f). In the CV analysis of PBS/2-NBA (curve e*), oxidation peak, Y, was seen to have shifted to a little higher potential (1.7 V). The reduction peak T (– 0.58 V) that was obtained could be attributed to the reverse deprotonation reaction as shown in Scheme 3.2 (path a'). In the CV analysis of CRS/2- NBA (curve f*), the reduction peak shifted to a slightly lower potential (– 0.65 V) with an increase in intensity, which

indicated that in the presence of creatinine, the feasibility of the reverse deprotonation reaction increased. The suppression of the oxidation peak, Q, resulted lowering of the intensity of the reduction peak, T, as can be seen in the CV analysis of CRS/2-NBA/NaOH (curve h*), which further inferred that the peaks, Q and T, are correlated. The occurrence of another reduction peak, U (-0.75 V), as observed in curve 'h*' could be attributed to the reverse deprotonation of oxalylmethylguanidine to yield creatol [Scheme 3.2 (path e')].

The mechanism proposed here is a plausible one which is partly corroborated by the findings of *Nakamura et al.* [30] in 1990. They reported the formation of a constitutional isomer of oxalylmethylguanidine, termed as Creatone A (2-Amino-1-methyl-4,5-imidazoledione) during oxidation of creatinine with mercury (II) acetate and confirmed its structure by 400 MHz ^1H NMR spectra [30]. They also conferred that formation of Creatone A occurred via another compound, termed as creatol (2-amino-5-hydroxy-1-methyl-1,5-dihydro-4 H-imidazol-4-one), and it wasn't the end product either. Under the action of mercury (II) acetate, creatinine also simultaneously got further oxidised to a zwitterionic compound, termed as Creatone B, and ultimately to other substituted guanidine compounds [30].

3.3.9.2 Spectroscopic support

Some FTIR analyses were also performed to gather evidence to validate certain aspects of the proposed mechanism. As all the FTIR spectra were recorded in the solution phase, the spectra obtained for the solvents alone had to be subtracted for appropriate analysis.

In Figure 3.11, it can be seen that when the spectrum obtained for ethanol (curve c) was subtracted from the spectrum obtained for the ethanolic solution of 2-Nitrobenzaldehyde (spectrum 'a'), it resulted in the spectrum denoted by spectrum 'd'. Three characteristic peaks of 2-NBA can be seen in spectrum 'd': at 1704 cm^{-1} which can be attributed to the stretching frequency of $\text{C}=\text{O}$; at 1536 cm^{-1} which can be attributed to the asymmetric stretching frequency of the nitro group and at 1349 cm^{-1} which can be attributed to the symmetric stretching of the nitro group [31]. But, when the spectrum of ethanol (curve c) was subtracted from the spectrum obtained for the mixture of ethanolic solution of 2-NBA and NaOH, it resulted in a spectrum denoted by curve 'e'. It can be seen in curve 'e' that no peak owing to the stretching frequency of $\text{C}=\text{O}$ appeared, while

the peaks for asymmetric and symmetric stretching of the nitro group shifted to slightly higher wavenumbers (1634 cm^{-1} and 1394 cm^{-1}). These shifts can be attributed to the effect of steric hindrance on the nitro group due to local environment change or H-bonding. Furthermore, broadening observed in the peaks due to symmetric and asymmetric stretching of the nitro group in curve 'e' could be attributed to conformational changes and H-bonding. Moreover, an additional peak obtained at 1041 cm^{-1} in curve 'e' can be attributed to C-O stretching [32]. These observations inferred the generation of 'Intermediate I' and 'Intermediate II' (that comprise C-O bonds and the nitro group in a more sterically hindered position) on the addition of NaOH to 2-NBA.

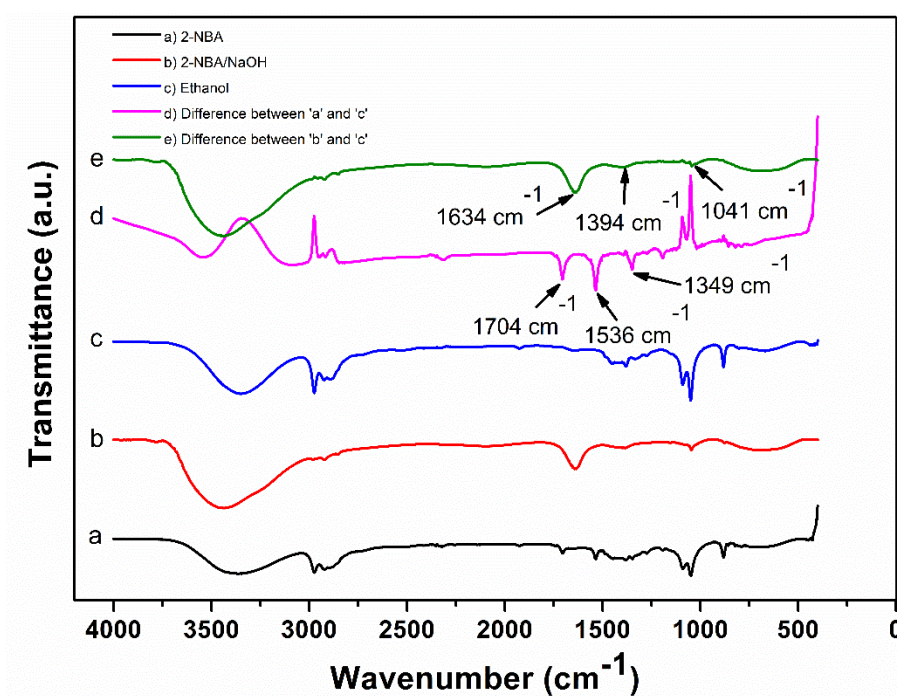


Figure 3.11: FTIR spectrum obtained for a) ethanolic solution of 2-NBA, b) 2-NBA/NaOH, c) ethanol, d) solvent (ethanol spectrum) removed spectrum 'a', and e) solvent (ethanol spectrum) removed from spectrum 'b'.

Figure 3.12 represents the FTIR spectrum obtained for the test solution, blank solution and PBS. It can be seen in the figure that the spectrum of PBS appears as the prominent one which masks the characteristic peaks in the other spectra.

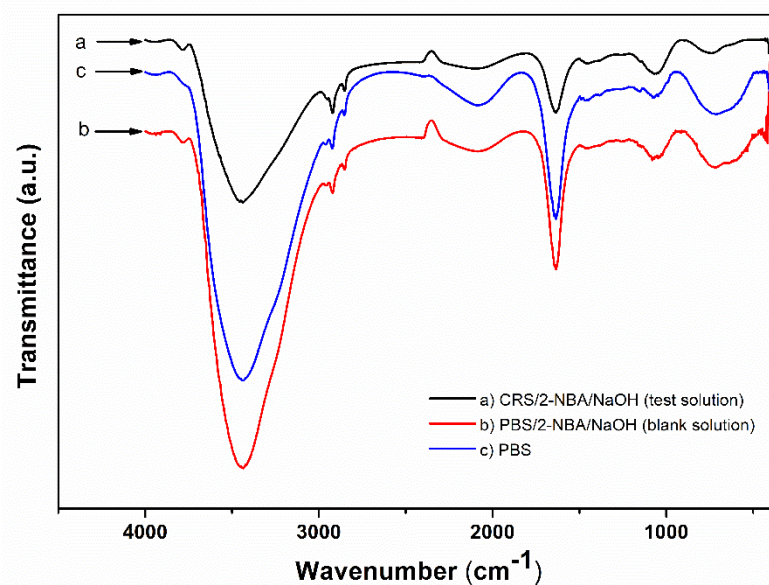


Figure 3.12: FTIR spectrum obtained for a) test solution (CRS/2-NBA/NaOH), b) blank solution (PBS/2-NBA/NaOH), and c) PBS.

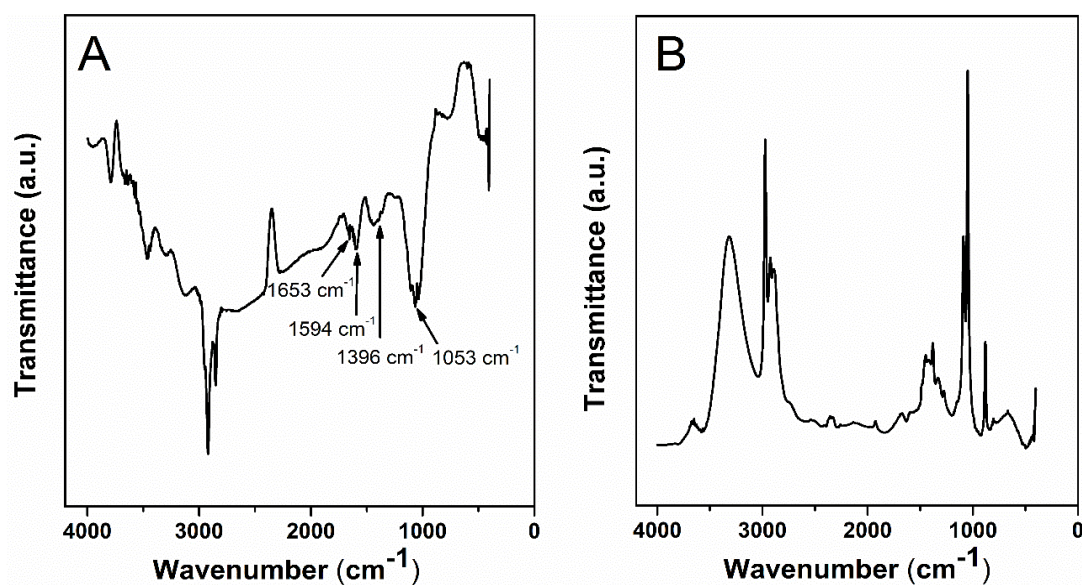


Figure 3.13: FTIR spectrum obtained for A) test solution, and B) blank solution, after subtracting the spectra of solvents.

When the spectra of the solvents (PBS and ethanol) were subtracted from the spectrum of the test solution, some characteristic peaks were observed as shown in Figure 3.13 (A). The peaks at 1594 cm^{-1} and 1396 cm^{-1} can be attributed to the asymmetric and

symmetric stretching of the nitro group. This infers the regeneration of 2-NBA from the 'Intermediate II-creatinine complex', in the test solution (regeneration of 2-Nitrobenzaldehyde was also confirmed by TLC). The peak at 1053 cm^{-1} can be attributed to the C-O (in the alcoholic group) stretching frequency. This infers the production of creatol. The peak at 1653 cm^{-1} can also be attributed to C = N stretching frequency, which is a characteristic peak of both creatol and creatinine.

However, when the spectra of the solvents (PBS and ethanol) were subtracted from the spectrum of the blank solution, no characteristic peak was observed as can be seen below in Figure 3.13 (B).

These observations also indicated a reaction between creatinine and 2-NBA in the presence of NaOH and fairly supported our proposed plausible mechanism.

3.4 Conclusion

We have successfully demonstrated an electrochemical urinary creatinine determination method based on the oxidation reaction of creatinine with 2-nitrobenzaldehyde/ethanol, in the presence of sodium hydroxide. Based on the electrochemical responses generated by DPVs and CVs, and corroborated by spectroscopic data, we have proposed a detailed mechanistic pathway of creatinine oxidation in this system. The detection and determination of creatinine level in a sample was accomplished with the DPV technique, after optimizing parameters like pH and reaction time. In the linear range of 1–25 mM, an excellent R^2 value of 0.99 was achieved and the LOD was determined to be 0.50 mM. Interference studies were carried out in the presence of other urinary components like urea, glucose, uric acid, dopamine and ascorbic acid, and overall, our process displayed a very good selectivity. Real sample analysis in human urine was successfully performed and recovery of spiked creatinine that was obtained in the range of 96.02–105.14 % also infers excellent sensitivity of the process. This electrochemical creatinine determination process requires neither tedious sample preparation nor intricate electrode modification, as it can be performed with bare GCE. Furthermore, it is an economical and time-efficient method. This is, in fact, a very novel approach involving a one-pot reaction for electrochemical creatinine detection, as it was accomplished by prior chemical conversion of creatinine to electroactive species, without the involvement of any enzyme or metal complex.

References

- [1] Jankhunthod, S., Kaewket, K., Termsombut, P., Khamdang, C. and Ngamchuea, K. Electrodeposited copper nanoparticles for creatinine detection via the in situ formation of copper-creatinine complexes. *Analytical and Bioanalytical Chemistry*, 415(16):3231–3242, 2023.
- [2] Mahmoud, A. M., Mahnashi, M. H. and El-Wakil, M. M. An innovative dual-signal electrochemical ratiometric determination of creatinine based on silver nanoparticles with intrinsic self-calibration property for bimetallic Prussian blue analogues. *Analytical and Bioanalytical Chemistry*, 415(25):6247–6256, 2023.
- [3] Kaewket, K. and Ngamchuea, K. Electrochemical detection of creatinine: exploiting copper (ii) complexes at Pt microelectrode arrays. *RSC Advances*, 13(47):33210–33220, 2023.
- [4] Kumar, R. K. R., Shaikh, M. O., Kumar, A., Liu, C. H. and Chuang, C. H. Zwitterion-functionalized cuprous oxide nanoparticles for highly specific and enzymeless electrochemical creatinine biosensing in human serum. *ACS Applied Nano Materials*, 6(3):2083–2094, 2023.
- [5] Ngamchuea, K., Wannapaiboon, S., Nongkhunsan, P., Hirunsit, P. and Fongkaew, I. Structural and electrochemical analysis of copper-creatinine complexes: application in creatinine detection. *Journal of The Electrochemical Society*, 169(2):020567, 2022.
- [6] Sato, N., Takeda, K. and Nakamura, N. Development of a Copper-electrodeposited Gold Electrode for an Amperometric Creatinine Sensor to Detect Creatinine in Urine without Pretreatment. *Electrochemistry*, 89(3):313–316, 2021.
- [7] Fava, E. L., do Prado, T. M., Garcia-Filho, A., Silva, T. A., Cincotto, F. H., de Moraes, F. C., Faria, R. C. and Fatibello-Filho, O. Non-enzymatic electrochemical determination of creatinine using a novel screen-printed microcell. *Talanta*, 207:120277, 2020.
- [8] Kalasin, S., Sangnuang, P., Khownarumit, P., Tang, I. M. and Surareungchai, W. Salivary creatinine detection using a Cu (I)/Cu (II) catalyst layer of a supercapacitive hybrid sensor: a wireless IoT device to monitor kidney diseases for

- remote medical mobility. *ACS Biomaterials Science & Engineering*, 6(10):5895–5910, 2020.
- [9] Gao, X., Gui, R., Guo, H., Wang, Z. and Liu, Q. Creatinine-induced specific signal responses and enzymeless ratiometric electrochemical detection based on copper nanoparticles electrodeposited on reduced graphene oxide-based hybrids. *Sensors and Actuators B: Chemical*, 285:201–208, 2019.
- [10] Raveendran, J., Resmi, P. E., Ramachandran, T., Nair, B. G. and Babu, T. S. Fabrication of a disposable non-enzymatic electrochemical creatinine sensor. *Sensors and Actuators B: Chemical*, 243:589–595, 2017.
- [11] Kumar, V., Hebbar, S., Kalam, R., Panwar, S., Prasad, S., Srikanta, S. S., Krishnaswamy, P. R. and Bhat, N. Creatinine-iron complex and its use in electrochemical measurement of urine creatinine. *IEEE Sensors Journal*, 18(2):830–836, 2017.
- [12] Riegert, A. Un nouveau microdosage colorimétrique de la créatinine, son application au plasma et au serum. *Comptes Rendus Société de Biologie*, 132:535, 1939.
- [13] Sakaguchi, S. Über eine neue Farbenreaktion von Protein und Arginin. *The Journal of Biochemistry*, 5(1):25–31, 1925.
- [14] Van Pilsum, J. F., Martin, R. P., Kito, E. and Hess, J., 1956. Determination of creatine, creatinine, arginine, guanidinoacetic acid, guanidine, and methylguanidine in biological fluids. *Journal of Biological Chemistry*, 222:225–236, 1956.
- [15] Jones, J. D. and Giovannetti, S. Charcoal-catalyzed oxidation of creatinine to methylguanidine. *Biochemical Medicine*, 5(3):281–284, 1971.
- [16] Nakai, T., Ohta, T., Obinata, Y. and Kojima, M. Air Oxidation of Creatine (or Creatinine) in strongly acidic solution: formation of Methylguanidine. *Agricultural and Biological Chemistry*, 42(4):891–892, 1978.
- [17] Manissorn, J., Fong-Ngern, K., Peerapen, P. and Thongboonkerd, V. Systematic evaluation for effects of urine pH on calcium oxalate crystallization, crystal-cell adhesion and internalization into renal tubular cells. *Scientific Reports*, 7(1):1798, 2017.

-
- [18] Liotta, E., Gottardo, R., Bonizzato, L., Pascali, J. P., Bertaso, A. and Tagliaro, F. Rapid and direct determination of creatinine in urine using capillary zone electrophoresis. *Clinica Chimica Acta*, 409(1-2):52–55, 2009.
- [19] Lewińska, I., Speichert, M., Granica, M. and Tymecki, Ł. Colorimetric point-of-care paper-based sensors for urinary creatinine with smartphone readout. *Sensors and Actuators B: Chemical*, 340:129915, 2021.
- [20] Chen, J. C., Kumar, A. S., Chung, H. H., Chien, S. H., Kuo, M. C. and Zen, J. M. An enzymeless electrochemical sensor for the selective determination of creatinine in human urine. *Sensors and Actuators B: Chemical*, 115(1):473–480, 2006.
- [21] Liu, L., Mo, H., Wei, S. and Raftery, D. Quantitative analysis of urea in human urine and serum by ^1H nuclear magnetic resonance. *Analyst*, 137(3):595–600, 2012.
- [22] Sechi, D., Greer, B., Johnson, J. and Hashemi, N. Three-dimensional paper-based microfluidic device for assays of protein and glucose in urine. *Analytical Chemistry*, 85(22):10733–10737, 2013.
- [23] Harris, L. J., Ray, S. N. and Ward, A. The excretion of vitamin C in human urine and its dependence on the dietary intake. *Biochemical Journal*, 27(6):2011, 1933.
- [24] Dalirirad, S. and Steckl, A. J. Lateral flow assay using aptamer-based sensing for on-site detection of dopamine in urine. *Analytical Biochemistry*, 596:113637, 2020.
- [25] Iwata, H., Nishio, S., Yokoyama, M., Matsumoto, A. and Takeuchi, M. Solubility of uric acid and supersaturation of monosodium urate: why is uric acid so highly soluble in urine? *The Journal of Urology*, 142(4):1095–1098, 1989.
- [26] Chauhan, N., Kumar, A. and Pundir, C. S. Construction of an uricase nanoparticles modified au electrode for amperometric determination of uric acid. *Applied Biochemistry and Biotechnology*, 174:1683–1694, 2014.
- [27] Sittiwong, J. and Unob, F. based platform for urinary creatinine detection. *Analytical Sciences*, 32(6):639–643, 2016.
- [28] Income, K., Ratnarathorn, N., Khamchaiyo, N., Srisuvo, C., Ruckthong, L. and Dungchai, W. Disposable Nonenzymatic Uric Acid and Creatinine Sensors Using μPAD Coupled with Screen-Printed Reduced Graphene Oxide-Gold Nanocomposites. *International Journal of Analytical Chemistry*, 2019(1):3457247, 2019.
-

-
- [29] Exner, O. and Böhm, S. Protonated nitro group: structure, energy and conjugation. *Organic & Biomolecular Chemistry*, 3(10):1838–1843, 2005.
- [30] Nakamura, K., Ohira, C., Yamamoto, H., Pfeleiderer, W. and Ienaga, K. Creatones A and B. Revision of the structure for the product of oxidation of creatinine and creatine. *Bulletin of the Chemical Society of Japan*, 63(5):1540–1542, 1990.
- [31] Pavia, D. L., Lampman, G. M., Kriz, G. S., and Vyvyan, J. A. *Introduction to Spectroscopy*. Cengage Learning, Boston, MA, 2008.
- [32] Mukhopadhyay, I., Ozier, I. and Lees, R. M. High-resolution spectrum of the C–O stretch overtone band in methyl alcohol. *The Journal of Chemical Physics*, 93(10):7049–7053, 1990.